Long Lasting Modifications to Vortex Shedding Using a Short Plasma Excitation

Timothy N. Jukes* and Kwing-So Choi†

Faculty of Engineering, University of Nottingham, Nottingham, NG7 2RD, United Kingdom

(Received 18 December 2008; published 22 June 2009)

A unique phenomenon in flow control is described, where the lift and drag on a circular cylinder could be modified for over eight vortex shedding cycles by a short pulse of dielectric-barrier-discharge plasma. This is equivalent to flow control for over 150 times the pulse duration, which seems to be due to a secondary vortex initiated by plasma that interacts with the von Kármán vortex formation and temporarily amplifies or suppresses the vortex street. Depending on the pulse timing, the drag and lift fluctuations could be increased by 22% and 50% or reduced by 8% and 40%, respectively, with a power saving ratio over 1000.

DOI: 10.1103/PhysRevLett.102.254501 PACS numbers: 47.32.ck, 47.85.L−, 47.85.lb

Periodic vortex shedding occurs for flow over bluff bodies [1] and results in large amplitude fluctuations in the aerodynamic forces [2]. This leads to structural vibrations which can have disastrous consequences. A plethora of effective strategies for periodic flow control exist which may be broadly categorized into passive or active techniques [3]. Passive techniques usually involve some sort of body modification or obstructions [4], such as surface protrusions, shrouds, and near-wake stabilizers like the well-known wake-splitter plate [5]. Active techniques require energy addition such as a rotational oscillation [6] or periodic momentum addition [7]. However, passive techniques can be detrimental when used off design conditions. For example, trip wires over a circular cylinder at subcritical conditions cause significant reductions in drag and lift coefficients with a shift in the Strouhal number [8], but the drag will increase with an increase in the Reynolds number due to the additional body surfaces acting as surface roughness. Active techniques, on the other hand, are rarely energy efficient and add complexities such as ducting and mechanical movement that may reduce the structural strength.

Dielectric-Barrier-Discharge (DBD) plasma actuators have recently become of interest to aerodynamicists as potential flow control devices [9] because they are simple and robust, have low power consumption, and a quick response. In this study, we use a single asymmetric DBD plasma actuator on a circular cylinder as shown in Fig. 1. The device consists of two electrodes (17 μm copper) separated by a dielectric layer (250 μm Mylar). High voltage ac is applied between the upper and lower electrodes ($E = 7.4$ kV$_{p\text{-}p}$, $f = 33$ kHz), which causes local ionization of the surrounding air so that plasma spreads over the surface. This appears as a light purple glow extending for approximately 3 mm (7°) to the downstream side of the upper electrode, under which the lower electrode is placed. A force, F_p, is generated by the plasma due to the free charges in a highly nonuniform electric field, which adds momentum to the ambient gas (net direction to the right in Fig. 1). For further details, including characteristics of the plasma induced flow and flow control applications, the reader should consult Refs. [9–14].

In this Letter, we describe a unique phenomenon whereby the vortex shedding and force fluctuations on a circular cylinder in cross flow are halted for considerably long duration by applying a single, short-duration pulse of DBD plasma close to flow separation points. This period is equivalent to flow modifications for over 150 times that of the excitation duration. We believe that this is a significant result for flow control from energy efficiency point of view.

Experiments were conducted in a low-speed open-return wind tunnel with test section of $1.5 \times 0.3 \times 0.3$ m. This was a suck-through-type tunnel located in a climate controlled laboratory. The free-stream velocity was $U_\infty = 4.6$ ms^{-1} at which the turbulence intensity was 0.5%. The circular cylinder tested had diameter $d = 50$ mm, length $l = 300$ mm, and the Reynolds number based on the cylinder diameter was 15 000. This corresponds to the transition-in-shear-layer flow state so that the boundary layers were laminar at separation. The transition to turbulence occurred shortly downstream and before the free shear-layers rolled up into a turbulent vortex street [15]. Vortex shedding took place at a reduced frequency $f_K{}^+ = d/T_K U_\infty = 0.22$, where T_K is the shedding period.

The cylinder model was mounted though the wind tunnel walls and into a two-component dynamic force balance. The balance consisted of two parallelograms

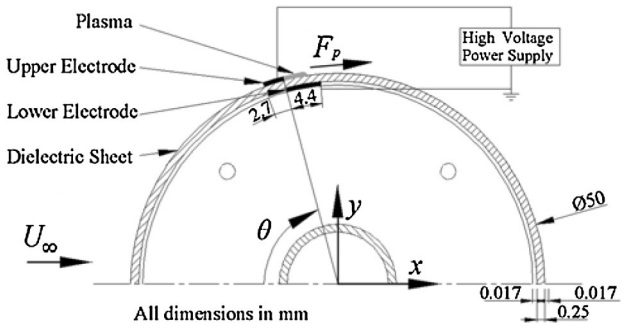

FIG. 1. Cylinder cross section. Electrodes drawn at 30:1 scale.

arranged in an L shape. Each parallelogram was instrumented with four strain gauges to measure the lift force, L, and drag, D, along the entire cylinder span. The overall accuracy in force measurement was better than ± 0.01 N (5%). The resonance frequencies were found to be 150 Hz ($f^+ = 1.67$) and 125 Hz ($f^+ = 1.39$) for lift and drag, respectively. This is more than 7 times the vortex shedding frequency. Simultaneously with the force measurements, the global flow field in the near wake was studied using a time-resolved particle image velocimetry (PIV) system from TSI. Flow measurements were taken at the cylinder midspan and PIV image pairs were taken at a frame rate of 1500 Hz, corresponding to 75 vector fields per vortex shedding period. Velocity vectors were computed on a square grid of edge size $0.028d$ using a recursive cross-correlation technique. Flow visualization was also performed using oil based smoke.

Force measurements were taken for a single pulse of DBD plasma of duration $\tau/T_K = 0.05$ (2.47 ms), at azimuthal location $\theta = 75°$ (cf. Fig. 1). We found this location gave the maximum effect on flow control and note that this is just upstream of the mean flow separation point at $\theta = 82°$ [15]. More than 230 measurements were made and phase-averaged into eight categories depending on the timing of the plasma pulse t_0 ($t_0 = 0$ indicates the plasma is fired at the time of maximum lift). PIV measurements were taken once for each phase for time $-0.5 \leq t/T_K \leq 1.5$, where $t = 0$ is the instant that the plasma turns on.

Figure 2 shows the flow response over the cylinder for different plasma timing. Clearly, the aerodynamic forces can be dramatically altered by a short plasma pulse, but their behavior depends on t_0. For example, it was possible to increase the peak lift by a factor of 3 while keeping the peak drag increase within 22% when plasma was fired to coincide with reducing L ($t_0/T_K = 0.375$). Alternatively, lift fluctuations could be reduced by 40% while drag was reduced by 8% when plasma fired as L increased ($t_0/T_K = 0.875$). In both cases, the modification lasted for more than eight vortex shedding periods, corresponding to flow alterations for over 150 pulse durations. The percentage change in mean drag and root-mean-squared lift fluctuations averaged over $0 \leq t/T_K \leq 8.5$ are shown as a function of t_0 in Fig. 3. Optimum timing occurred at $t_0/T_K = 0.875$, where drag coefficient $C_D = 2D/\rho U_\infty{}^2 dl$ and lift fluctuation coefficient $C_L' = 2L'/\rho U_\infty{}^2 dl$ reduced by 5.8% and 41%, respectively ($'$ denotes root-mean-squared quantity).

The operation of flow control is shown in the PIV and flow visualization images in Fig. 4 at the optimum pulse timing ($t_0/T_K = 0.875$: plasma initiated just before peak lift). Frame (i) shows the flow before plasma fires, where shear-layer transition vortices [16] can be seen shortly downstream of separation ($x/d = 0.5$, $y/d = 0.6$). When the plasma activates, momentum is added to the boundary layer on the upper surface of the cylinder [frame (ii)]. This causes a break between the reattached boundary layer and the shear layer that has already been separated so that the tail of the old shear layer rolls up as it moves downstream

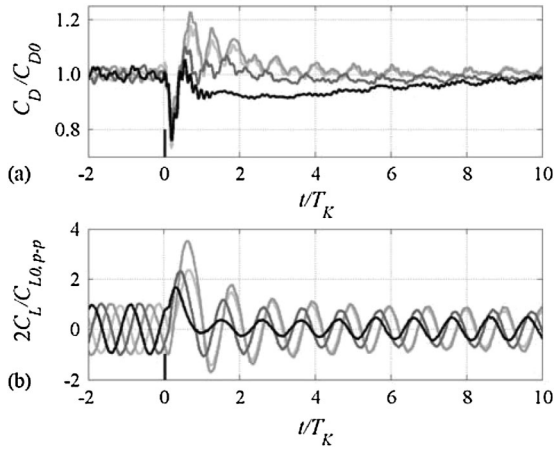

FIG. 2. Phase-averaged response to a single pulse of DBD plasma at $\theta = 75°$ for $\tau/T_K = 0.05$. (a) Normalized drag coefficient; (b) Normalized lift coefficient. Plasma pulse timing and duration shown on abscissa. Traces show response for different plasma timing relative to vortex shedding cycle.

[frame (ii), $x/d = 0.4$, $y/d = 0.6$]. The reenergized boundary layer now has sufficient momentum to overcome the adverse pressure gradient on the rear of the cylinder and to remain attached to around $\theta = 120°$ [frame (iii)]. This forms a secondary vortex [frame (iv–vi)], containing the vorticity added by the plasma [see frame (v) at $x/d = 0.5$, $y/d = 0.4$]. The secondary vortex is then convected into the near wake.

This formation process of the secondary vortex was independent of the plasma timing relative to the vortex shedding cycle. The role of t_0 is therefore only to change the timing of releasing the secondary vortex into the wake. Figure 5 illustrates this point where the near wake flow is shown at various time steps for optimum plasma timing $t_0/T_K = 0.875$. Figures 5(a) and 5(b) show the near wake before the plasma initiates. These images are separated in time by one-half the vortex shedding cycle so that the natural vortex shedding cycle is demonstrated. Gerrard [17] defined the vortex being shed from the cylinder when it becomes strong enough to draw the other shear layer across the wake, cutting it off from further supply of

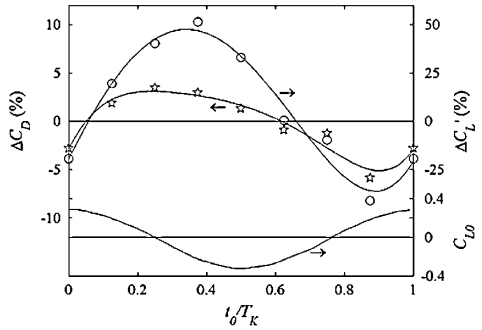

FIG. 3. Change in mean drag and lift fluctuations over 8.5 shedding periods after plasma as a function of actuation timing, t_0/T_K. C_{L0} is the instantaneous lift coefficient when plasma fires.

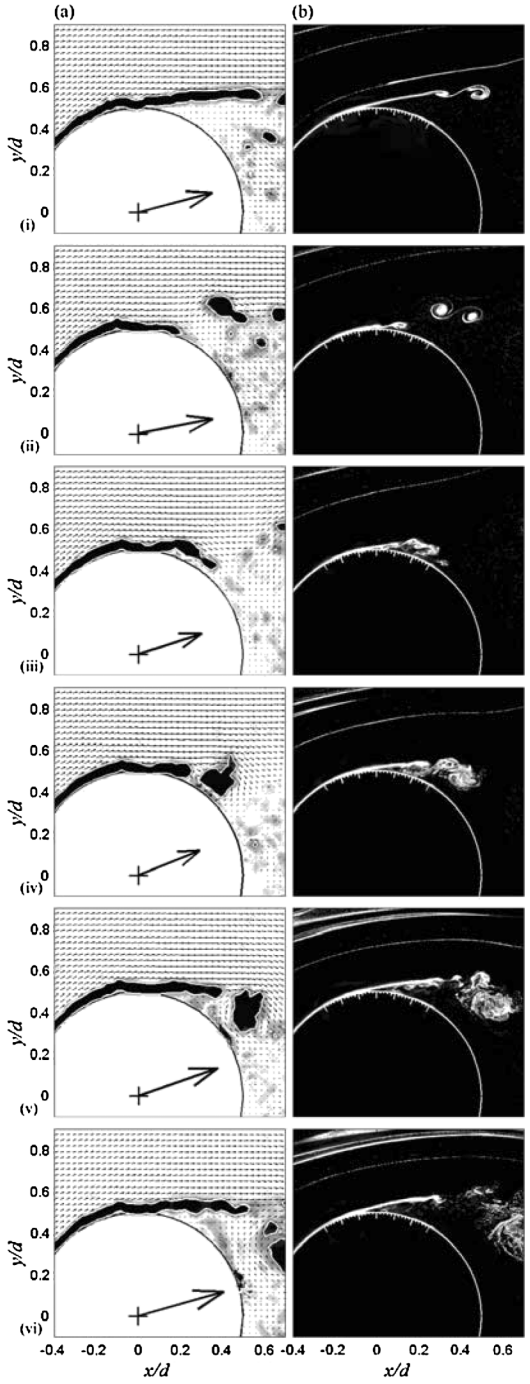

FIG. 4. (a) Vorticity contour and force vector (shown by arrow); (b) flow visualization around upper surface of the cylinder. Plasma activated at time $t_0/T_K = 0.875$, at location $\theta = 75°$ with duration $\tau/T_K = 0.05$. Dark areas in (a) mark $\Omega_z d/U_\infty < -17$ (clockwise rotation). Time increments down page: $t/T_K = -0.01, 0.10, 0.20, 0.30, 0.40, 0.50$.

circulation. Based on this definition and the observations by Drescher [18], vortices are shed from the upper and lower surfaces of the cylinder in Fig. 5 at times $t/T_K = -0.625$ and -0.125, respectively. Thus, Fig. 5(a) shows the flow shortly before the upper vortex detaches while (b) shows the flow before the lower vortex detaches.

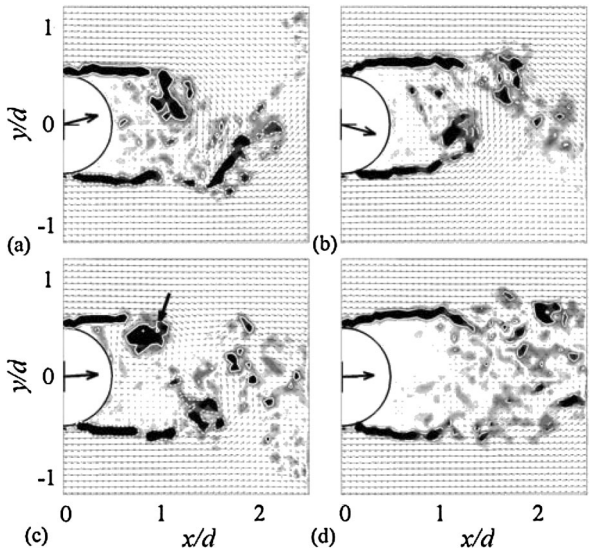

FIG. 5. Vorticity contours with instantaneous force vector. Solid contours mark $\Omega_z d/U_\infty = -17$ (clockwise rotation) while dashed contours mark $\Omega_z d/U_\infty = +17$ (counterclockwise rotation). Plasma activated at time $t_0/T_K = 0.875$, at location $\theta = 75°$ with duration $\tau/T_K = 0.05$. (a) $t/T_K = -0.8$; (b) $t/T_K = -0.3$; (c) $t/T_K = 0.7$; (d) $t/T_K = 2.7$.

Figure 5(c) shows the flow at $t/T_K = 0.7$ after plasma fires, when the secondary vortex with negative vorticity is being released into the wake (marked by an arrow in the wake region). This frame is exactly one shedding period after Fig. 5(b) to highlight the difference in the wake structure with the addition of this secondary vortex. The lower shear layers in (c) and (b) are quite similar, so that the vortex is released from the upper surface while the vortex from the lower surface is still being formed. The secondary vortex thus counteracts the entrainment process at the lower part of the cylinder. This halts the vortex shedding, or moves it far downstream so that the cross-flow oscillations do not cause lift force fluctuations. Figure 5(d) shows the flow 2.7 vortex shedding periods after the plasma pulse. The wake is nearly symmetrical and the shear layers seem to detach parallel to the free-stream flow and equally from the upper and lower surfaces. Very little cross-wake interactions are observed here, and there is no sign of a vortex street in the near wake. This flow field remains for about 4 to 5 vortex shedding periods after the plasma excitation. Thereafter, a wake oscillation was observed in the downstream region, which slowly proceeded upstream until vortex shedding recommenced and normal flow conditions were restored.

Alternatively, the secondary vortex could be released after the vortex from the lower cylinder surface had detached ($t_0/T_K \approx 0.375$). Then the additional vorticity was injected into the newly forming vortex from the upper surface to increase its strength. This enhanced the vortex shedding process and the vortex formation region moved upstream and closer to the cylinder for the next 4–5 vortex

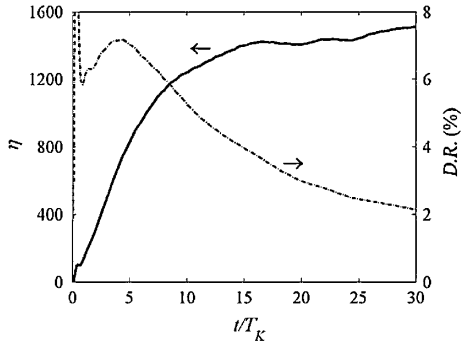

FIG. 6. Power saving ratio and time-averaged drag reduction as a function of time between plasma control pulses.

shedding periods. This increased the lift fluctuations as well as the drag (cf. Fig. 2).

The power saving ratio of the present flow control strategy, η, can be defined as a ratio of the power saved by drag reduction, $\Delta D U_\infty$, to the fluidic power introduced by the plasma, $\lambda F_p l U_\infty$. Here, λ is the plasma duty cycle defined as a time fraction of plasma actuation during the flow control. The plasma induced body force was estimated from momentum theory using PIV measurements in still air to be $F_p = 6.6 \times 10^{-3}\ \mathrm{N\,m^{-1}}$. Figure 6 shows the variation of η and mean drag reduction with time between control pulses when plasma was activated at $t_0/T_K = 0.875$. The initial peak in drag reduction is due to the formation and release of the secondary vortex (cf. Fig. 2). The power-saving ratio of this control strategy plateaus at $\eta \approx 1500$ for $t/T_K > 15$ although the mean drag reduction drops off for $t/T_K > 5$. A suitable control strategy would be to reactivate plasma every $8.5T_K$ ($\lambda = 0.59\%$), which results in mean drag reduction of 5.8%. The power saving ratio of this control strategy would be as much as $\eta = 1170$. Compare this to a power saving ratio of order 10 for drag reduction on a circular cylinder by rotational oscillation [19]; the Kim-Choi [20] distributed forcing by suction and blowing gives $\eta = 150$, which is still an order of magnitude smaller than that of the present control strategy.

The effectiveness of plasma in reducing drag can also be expressed in terms of the energy efficiency, η_e, which is defined as a ratio of the power saved by drag reduction to the electrical power applied to the actuator (measured from voltage and current waveforms). The control strategy described above, where the plasma is reactivated every $8.5T_K$ ($\lambda = 0.59\%$), gives the energy efficiency of $\eta_e = 51\%$. Here, neither η nor η_e incorporates any saving due to reductions in lift fluctuations which may be more important than drag reduction for some applications. We expect the energy efficiency η_e could be improved through optimization of the actuator design and the high voltage power supply.

In conclusion, we discovered that a single, short-duration actuation of DBD plasma modified the vortex shedding cycle from a circular cylinder for over 150 times the pulse duration. The flow control for such a long duration seems to be due to the induced secondary vortex by plasma that interacted with the von Kármán vortex formation, where the drag and lift fluctuations can be reduced by 8% and 40%, respectively. The power-saving ratio could be as much as 1170, while the energy efficiency was 51%. As such, our result has important implications for flow control strategies and great potential for industrial applications.

We gratefully acknowledge support by EPSRC Grant No. EP/D500850/1. We also thank M. Hyde of TSI and the EPSRC Engineering Instrument Pool for use and advice with the high-speed PIV system. Thanks are also given to S. Scott and G. Johnson of BAE SYSTEMS for the use of the high voltage power supply.

*Author to whom correspondence should be addressed: Kwing-So.Choi@nottingham.ac.uk.
†Timothy.Jukes@nottingham.ac.uk.

[1] E. Berger and R. Wille, Annu. Rev. Fluid Mech. **4**, 313 (1972).
[2] C. Norberg, J. Fluids Struct. **17**, 57 (2003).
[3] M. Gad-el-Hak, *Flow Control: Passive, Active, and Reactive Flow Management* (Cambridge University Press, Cambridge, England, 2000).
[4] M. M. Zdravkovich, J. Wind Eng. Ind. Aerodyn. **7**, 145 (1981).
[5] A. Roshko, J. Wind Eng. Ind. Aerodyn. **49**, 79 (1993).
[6] P. T. Tokumaru and P. E. Dimotakis, J. Fluid Mech. **224**, 77 (1991).
[7] D. Greenblatt and I. J. Wygnanski, Prog. Aerosp. Sci. **36**, 487 (2000).
[8] F. S. Hover, H. Tvedt and M. S. Triantafyllou, J. Fluid Mech. **448**, 175 (2001).
[9] E. Moreau, J. Phys. D **40**, 605 (2007).
[10] T. N. Jukes, K.-S. Choi, G. A. Johnson and S. J. Scott, AIAA J. **44**, 764 (2006).
[11] J. R. Roth and D. M. Sherman, AIAA J. **38**, 1166 (2000).
[12] F. O. Thomas, A. Kozlov, and T. C. Corke, AIAA J. **46**, 1921 (2008).
[13] M. Post and T. Corke, AIAA J. **44**, 3125 (2006).
[14] T. N. Jukes, K.-S. Choi, G. A. Johnson, and S. J. Scott, *3rd AIAA Flow Control Conference, San Francisco, CA* (AIAA Report No. 2006-3693, 2006).
[15] M. M. Zdravkovich, *Flow Around Circular Cylinders* (Oxford University Press, New York, 1997), Vol. 1.
[16] S. M. Bloor, J. Fluid Mech. **19**, 290 (1964).
[17] J. H. Gerrard, J. Fluid Mech. **25**, 401 (1966).
[18] H. Drescher, Z. Flugwiss. Weltraumforsch **4**, 17 (1956).
[19] D. Shiels and A. Leonard, J. Fluid Mech. **431**, 297 (2001).
[20] J. Kim and H. Choi, Phys. Fluids **17**, 033103 (2005).